EURASIAN JOURNAL OF MATHEMATICAL AND COMPUTER APPLICATIONS
ISSN 2306–6172
Volume 12, Issue 4 (2024) 158 – 174

NUMERICAL SIMULATION OF THERMAL GRAVITATIONAL-CAPILLARY CONVECTION IN EXTRA THIN LIQUID LAYERS

Vinokurov V.V., Vinokurov V.A., Marchuk I.V., Kabov O.A.

Abstract Numerical solutions of the three-dimensional equations for Rayleigh-Benard convection in extremely thin layers of different liquids (water and Fluorinert Electronic Liquid FC-72 coolant) uniformly heated from below are presented. The relative size of the liquid layer $\Gamma = D/H$ varied from 8 to 400. The sizes of ordered Rayleigh-Benard convective cells were determined, which for water are about 0.42 mm with a layer diameter of 40 mm and a layer height of 0.4 mm, which is comparable with the minimum experimentally recorded transverse size of a monolayer of hovering microdroplets above an evaporating liquid layer in the atmosphere. The effect of temperature difference and liquid layer height on heat transfer was studied. The relative contribution of buoyancy forces and the thermocapillary effect was investigated. The temperature difference at which the transition to non-stationary flow regimes occurs was determined for water. Analytical approximations of the integral heat flux from the free surface of the liquid layer are presented.

Key words: Rayleigh - Benard convection, numerical modeling, levitating microdrops, thermogravitational convection, thermocapillary convection, heat transfer.

AMS Mathematics Subject Classification: 76R10.

DOI: 10.32523/2306-6172-2024-12-4-158-174

1 Introduction

Microdroplets are used in various of engineering and technology branches such as the spread of fertilizers and pesticides, fire extinguishing, inkjet printers, 3D printing, IC engines and rocket engines, thin-film coatings, cooling chips in microelectronics and much more [1]. Microdroplets are important in the spread of viruses, as well as in the delivery of drugs to the lungs [2,3,4]. Levitating microdroplets at sufficiently low temperatures can have a significant impact on the efficiency of cooling systems and other technologies [5]. When a liquid layer evaporates near the liquid-gas interface, microdroplets ordered in a hexagonal structure can be observed. In 1971, Schaefer [6] published a paper where he described the mechanism of formation of a layer of white mist over a cup of hot coffee. This mechanism of droplet formation is associated with an upward flow of vapor over a heated liquid surface, as well as transport phenomenon called Stefan's flow. The liquid evaporates and the vapor rises into an area of lower temperatures, where it condenses. The microdroplets move downwards until the gravity force is balanced by the force arising from the flow of the vapor-air mixture rising from below. Eventually, the droplets begin to levitate above the surface of the heated liquid. Here, the Stefan's flow is a macroscopic movement of moist air, compensating

for the diffusion of air molecules to the evaporating surface of the liquid [7]. The same phenomenon occurs during stationary condensation.

Thirty years later, in [8] a similar phenomenon was discovered in the study of photoinduced thermocapillary flows, which was called a droplet cluster. A heat source with a diameter of 1 mm was used in the experiments. It was experimentally shown that the velocity of the vapor flow from the liquid surface is sufficient to compensate for the force of gravity acting on the droplet, and it begins to levitate [9]. In addition, it was found that the droplet cluster "disappears" in just 3 ms as a result of the propagation of a capillary wave [10,11]. The studies were carried out using local heating of an area of 1x1 mm2. This phenomenon can also be observed over a number of heated liquids, such as glycerol and benzyl alcohol. The droplet size can vary from a few microns to 0.05-0.1 mm and increases as the temperature of the evaporating liquid increases. The levitation height of the droplet is comparable to the size of the droplet. The "lifetime" of the monolayer can be minutes, and in some cases, hours.

There are relatively few computational works on the topic of levitating droplets. A mathematical model of droplet levitation above a layer of evaporating liquid was developed in 2017 [12]. An analytical formula was developed for the levitation height depending on the droplet diameter. The study [13] already takes into account the final size of condensing droplets. Davis et al. [14] recently developed a comprehensive theory that is able to predict both the levitation height and the evolution of the droplet diameter.

Self-assembled levitating monolayer of microdroplets have been observed above a heated surface using a heat source of $D = 1.6$ mm [15], $D = 3$ mm [16], 10×10 mm [12,17,18], and also using a heat source with a diameter of 12 mm [19]; In experiments with heaters of $1 \times 1\,\text{mm}^2$, $D = 1.6$ mm and $D = 3$ mm, a levitating monolayer of microdroplets was formed and it could cover almost the entire heater at sufficiently high temperatures of the liquid layer. In experiments with heaters of $10 \times 10\,\text{mm}^2$ and $D = 12$ mm, the monolayer size was always significantly smaller than the heater size and did not exceed 2.8 mm. In this case, large ordered arrays of microdroplets move chaotically over the heating surface as a single whole and can include up to 10 thousand or more microdroplets.

There are no systematic studies explaining the possible influence of convection in a layer of evaporating liquid on the dynamics of a levitating monolayer of microdroplets nowadays. In this and many other natural phenomena, thermal gravitational-capillary convection plays an important role [20]. With significant non-isothermality of the system and with the dependence of the density of the fluid on temperature, buoyancy forces (Archimedes' force) are fundamentally unavoidable under terrestrial conditions. As a result, in any of these systems located in a gravity field, the basic convective flow will be thermogravitational convection. Another type of thermal convection is thermocapillary convection, which takes place as a result of uneven heating of the liquid surface; it is of a near-surface nature and, as a rule, does not involve deep layers of liquid or gas in movement [21]. In conditions of the absence of gravity, for example, on the International Space Station, thermocapillary convection is of decisive importance.

Rayleigh-Benard convection in horizontal layers of liquid heated from below [22,23]

is a classical problem of scientific research. The resulting Rayleigh-Benard cells are ordered large-scale structures in the form of cylindrical shafts. With a solid, uniformly cooled upper boundary, only thermogravitational convection occurs in the system; if the boundary is free, then combined thermal gravitational-capillary convection occurs. The main dimensionless parameters in problems with Rayleigh-Benard convection are the Rayleigh (Ra), Marangoni (Ma) (if there is a free upper boundary) and Prandtl (Pr) numbers.

Systematic experimental studies of Rayleigh-Benard convection were presented in [24,25,26] and were aimed at studying the relative contribution of buoyancy forces and the thermocapillary effect, as well as studying laminar-turbulent transitions. In particular, these studies showed that when approaching the critical number Racr, when the transition from one type of flow to another occurs, successive changes in the local heat flux are observed [25]. The studies were conducted for turbulent regimes with Rayleigh numbers Ra=$10^7 - 10^8$. In [26], where a horizontal layer of alcohol (Pr=16) measuring 240 × 240 mm and a height of 2 to 30 mm was studied, information on temperature gradients on the free surface in stationary and non-stationary modes was obtained using a thermal imager. In layers of 1-2 mm hight, classical 6-sided Rayleigh-Benard cells were formed, and when the layer height increased to 6 mm, polygonal cells were formed.

In 2010 [27], using direct numerical modeling, the influence of the relative size of the cylindrical layer ($\Gamma = D/H$, $0.5 \leq \Gamma \leq 12$) and the Rayleigh number ($10^7 \leq \mathrm{Ra} \leq 10^9$) on the formation of spatial structures of Rayleigh-Benard convection at a fixed number $\mathrm{Pr} = 0.7$ was presented. The dependence of the Nusselt number on the relative cell size $\mathrm{Nu}(\Gamma)$ was found. The minimum Nusselt values corresponded to the regimes $\Gamma \approx 2.5$, $\mathrm{Ra} = 10^7$ and $\Gamma \approx 2.25$, $\mathrm{Ra} = 10^8$. The results of numerical simulation of turbulent Rayleigh-Benard convection for the aspect ratio (diameter/height) $\Gamma = 1.0$, Prandtl numbers of 0.4 and 0.7, and Rayleigh numbers from $10^5 \leq \mathrm{Ra} \leq 10^9$ were presented in [28]. Detailed measurements of the thermal and viscous boundary layer profiles were carried out and compared with experimental and theoretical (Prandtl-Blasius [29]) results. It was found that the thermal boundary layer profiles do not coincide with the theoretical Prandtl-Blasius results. At the same time, the profiles of the viscous (hydrodynamic) boundary layer are in good agreement with the theoretical Prandtl-Blasius profiles (within 10%). Dependences of the boundary layer thickness on the Rayleigh number are obtained.

In [30], the Rayleigh-Benard convection was investigated for Rayleigh numbers up to 10^9 in a rectangular cavity using asymptotic and numerical methods. Comparisons of these two methods showed good agreement. The Rayleigh values and the coefficient $\lambda = W/Hb$ (W is the width, Hb is the height of the Benard cells) for which stationary solutions exist were determined. In [31], devoted to direct numerical modeling of convection in a cylindrical cell ($\Gamma = 6.3$), convection was studied at Rayleigh numbers of $9.6 \cdot 10^7$ and a fixed number $\mathrm{Pr} = 6.7$. For different time intervals, instantaneous fields of temperature and vertical velocity component in the cross-section along the cell height $H/2$ were presented. In 2020 [32], the Fourier method was used to study coherent structures and turbulent Rayleigh-Benard convection.

Based on the Navier-Stokes equations in the Boussinesq approximation [33], the

effect of the Prandtl number (Pr = 0.005 − 70) on the three-dimensional flow structure with relative cell sizes of 25:25:1 (Γ = layer length L/layer height H = 25) was numerically investigated for Rayleigh numbers up to 10^7. The calculations showed the existence of cylindrical rolls in unsteady turbulent regimes. Richard et al. [34] numerically investigated large-scale and long-lived coherent structures in highly turbulent Rayleigh-Benard convection for Ra $\leq 10^9$ in a horizontal cell. The effect of the ratio $\Gamma = D/H$ on the convection structure was also studied. In some regimes, large-scale structures had horizontal sizes of $(6-7)\cdot H$. In [35], turbulent convection in a cylindrical container heated from below with a relative diameter of $\Gamma = D/H = 1$ was studied numerically. It was shown that a small tilt of the container axis by only 2 degrees relative to the gravity vector leads to fixation of the global vortex of large-scale circulation in the azimuthal position. Calculations were performed for water (Pr = 6.4) and mercury (Pr = 0.025), as well as for the numbers Ra = 10^8 and Ra = 10^6, respectively.

In [36], a new model of large eddy simulation (LES) was implemented for numerical studies of Rayleigh-Benard convection at extreme Rayleigh numbers $10^6 \leq$ Ra $\leq 10^{13}$, Pr = 0.768 and 1.0, $\Gamma = 10$. The aim of the work is to investigate the physics of convective flow at very high Rayleigh numbers. In particular, the dependences of Nusselt numbers on Ra were presented. Zhou and Chen [37] numerically studied large-scale structures of turbulent Rayleigh-Benard convection in a thin rectangle ($\Gamma = 6$) using direct numerical simulation, Pr = 0.7, $10^7 \leq$ Ra $\leq 5 \cdot 10^9$. A fixed temperature was specified at the upper and lower boundaries, and the adiabatic condition was specified on the side walls. An analytical dependence of the Nusselt number on the Rayleigh number Nu $\sim 0.138 \cdot$ Ra$^{0.3}$, as well as velocity profiles in the boundary layers, were presented. In the work [38], devoted to the Rayleigh-Benard convection, the transition to the so-called limiting regime, in which both the volume and the boundary layers are turbulent, was investigated. The authors claim that by performing two-dimensional numerical modeling of the Rayleigh-Benard flow up to the Rayleigh number Ra $\leq 10^{14}$ ($Pr = 1$, $\Gamma = W/L = 2$, where W is the width of the region), the transition to the limiting regime at Ra = 10^{13} was found for the first time. Also, an analytical dependence of the Nusselt number on the Rayleigh number was found: Nu $\sim$ Ra$^{0.38}$.

Despite the fact that Rayleigh-Benard convection has been studied for a long time both experimentally and numerically for very thin cylindrical liquid layers ($\Gamma > 100$), in the range of small Ra and Ma numbers, thermal gravity-capillary flow has not been fully studied. This work is devoted to numerical 2D and 3D modeling of convection in extremely thin cylindrical liquid layers with a free surface (the aspect ratio Γ reaches 400), uniformly heated from below. The study was performed for water ($2.15 \leq$ Pr $\leq$ 2.40, depending on temperature) and for the coolant Fluorinert Electronic Liquid FC-72 (Pr=2.13). This work is one of the stages of the study of the possible connection between the emergence, development and dynamics of a "droplet cluster" levitating above a horizontal liquid-gas interface at a distance comparable to the droplet diameter, and the structure of convective flows in an evaporating liquid layer. This article is a continuation of the work on the study of convective flow in extremely thin cylindrical layers [39]. In our new work, we compare the sizes of convective cells, integral heat flows for different liquids (water and Fluorinert Electronic Liquid FC-72) in order to better understand the patterns of convective flow and heat exchange in very thin liquid

layers.

The aim of the research is to study the relative contribution of the temperature gradient, liquid layer height, liquid properties with different Prandtl numbers, buoyancy forces and thermocapillary effect to the formation of the flow structure and heat transfer observed in thin liquid layers heated from below. In this paper, only thermal gravity-capillary convection in a thin liquid layer is considered. Transfer processes in a gaseous medium are not taken into account.

2 Physics-mathematical formulation of the problem

The computational domain is a cylinder with a height of $0.1\,\text{mm} \leq H \leq 5\,\text{mm}$ and a diameter of $D = 10 - 40$ mm. Thus, the relative size of the liquid layer height $\Gamma = D/H$ varied from 8 to 400. The ranges of diameters and heights of the liquid layer were chosen to be typical for experimental studies in which a monolayer of levitating water microdroplets above the surface of a heated liquid layer was studied [17,19]. In addition, as mentioned above, convective flow in very thin cylindrical liquid layers with $\Gamma = D/H > 100$ has not been studied in detail to date.

Numerical 2D and 3D modeling of convection are carried out using the Ansys Fluent software package. Physical coordinates x, y, z were used in the three-dimensional case and x, y in the two-dimensional case. The two-dimensional problem statement was used in stationary modes, and the three-dimensional problem statement was used in non-stationary modes. One of the reasons for the combined use of 2D and 3D problem statements is to verify the accuracy of the numerical calculation. For this purpose, the integral heat flux from the free surface of the liquid was controlled. The results obtained coincided.

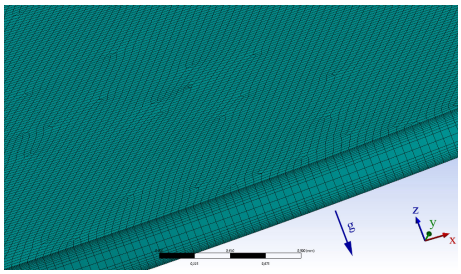

Figure 1: Enlarged fragment of the computational mesh

The Ansys Fluent software package is based on solving the Navier-Stokes equations using the control volume method. The number of cells in the computational grid in the 3D formulation varied from 10 million to $\sim$ 14.8 million depending on the height of the liquid layer. The 3D grid is generated in Ansys Meshing using the MultiZone grid method (Fig. 1).

The computational mesh was generated with an inflation layers at the top and bottom of a thin cylinder layer for more accurate determination of local and heat fluxes. The inflation parameters were as follows: *Growth Rate*=1.2, *Maximum Layers*=5, *Transition Ratio*=0.3. The computational mesh quality is controlled by the mesh metrics: *Skewness*=0.031, *Orthogonal quality*=0.98. *Orthogonal quality* during

mesh generation can vary from 0 to 1.0, this is an indicator that measures how well the mesh elements are aligned with the flow direction. High orthogonality (1.0) means that the mesh faces are perpendicular to the flow, which is highly desirable for the accuracy and convergence of the solution. The manual for the Ansys Fluent Range software package states that the *Skewness* parameter for excellent mesh quality must be 0-0.25. The smaller the better. In our case, *Skewness*=0.031, which indicates a very high quality of the constructed computational mesh.

The motion of the fluid is described by the Boussinesq approximation of the Navier-Stokes equations:

$$\frac{\partial \vec{U}}{\partial t} + (\vec{U} \cdot \nabla)\vec{U} = -\frac{1}{\rho_0}\nabla p + \nu \Delta \vec{U} - \beta T \vec{g}, \quad \frac{\partial T}{\partial t} + \vec{U} \cdot \nabla T = \alpha \Delta T, \quad \mathrm{div}\vec{U} = 0.$$

Vector $\vec{g}$ acts in the negative z direction (Fig. 1). Here U (U_x, U_y, U_z) is the flow velocity, T is the temperature, t is the time, p is the pressure, g is the acceleration due to gravity, β is the coefficient of volumetric expansion, ρ_0 is the density of the liquid at some temperature T_0. The Ansys Fluent software package has a section of reference values, where the value $T_0 = (T_2 + T_1)/2$, i.e. this is the average temperature in the liquid layer, and ρ_0 is the corresponding density of the liquid. The boundary conditions for numerical modeling are as follows. There is a cylindrical vessel filled with liquid. At the bottom of the cylindrical vessel ($z = 0$) the temperature T_1 is set. On the side walls of the cylinder, the thermal insulation condition is set, i.e. the absence of heat flux $\partial T/\partial n = 0$. The temperature on the free surface ($z = H$) is constant $T = T_2$, where $T_1 > T_2$. On all boundaries, except for the free surface, the adhesion conditions are satisfied, this indicates that the liquid adheres to the wall and moves with the same speed as the wall ($U = 0$). The free surface is flat, non-deformable and motionless in the z direction. Also on the free surface at $z = H$, the condition of balance of the tangential component of the force caused by the gradient of surface tension and friction forces is set:

$$\mu \frac{\partial \vec{U}}{\partial z}\bigg|_{z=H} = -\frac{\partial \sigma}{\partial T}\frac{\partial T}{\partial r}.$$

Here is the derivative of the surface tension coefficient with respect to temperature from $(x, y, z = H)$ to $(0, 0, z = H)$. μ is the dynamic viscosity. The following initial conditions for velocity and temperature are used (in the initialization of the Ansys Fluent software package): $U_x = 0$, $U_y = 0$, $U_z = 0$, $T = T_1$, $p = 0$. The acceleration of gravity is $g = 9.81\,\mathrm{m/s^2}$. σ is the surface tension coefficient, ν is the kinematic viscosity, α is the thermal diffusivity. The thermophysical characteristics of water were taken from the data in [40]. The dimensionless defining parameters of the problem are the Rayleigh, Grashof, Marangoni and Prandtl numbers:

$$\mathrm{Ra} = \frac{g\beta}{\nu\alpha}\Delta T \cdot H^3, \quad \mathrm{Gr} = \frac{g\beta}{\nu^2}\Delta T \cdot H^3, \quad \mathrm{Ma} = -\frac{\partial \sigma}{\partial T}\frac{H}{\alpha\mu}\Delta T, \quad \mathrm{Pr} = \frac{\nu}{\alpha}.$$

An important issue is the control of the accuracy of numerical simulation. One of the effective ways to check the correctness of the obtained solution is to check the balance of the integral heat flux through the heated (bottom of the cylindrical region) and cold (free surface) boundary of the cylinder. Taking into account the boundary conditions for temperature, $Q_1 = Q_2$ must be satisfied, i.e. the equality of the integral heat fluxes at the bottom of the cylindrical layer of liquid (T_1 is the temperature at the bottom,

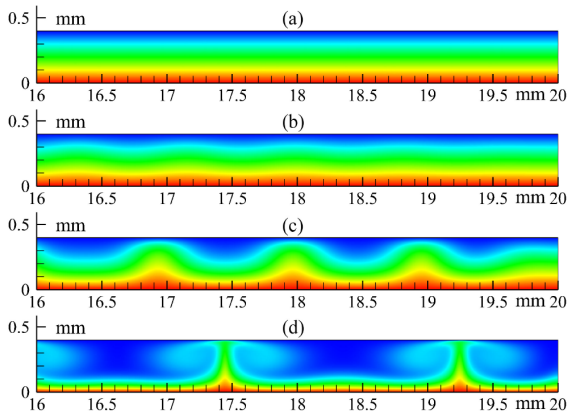

Figure 2: Fluorinert Electronic Liquid FC-72. $\Gamma = D/H = 100$. Temperature isolines $T(x, z)$ in the section of the plane $y = 0$. Stationary modes. a) $\Delta T = 3.0°$C, Gr = 20.3, Ma = 5371; b) $\Delta T = 3.1°$C, Gr = 21, Ma = 5550; c) $\Delta T = 3.2°$C, Gr = 21.7, Ma = 5730; d) $\Delta T = 10.0°$C, Gr = 68, Ma = 17903.

Q_1 is the corresponding calculated heat flux) and on the free surface of the liquid (T_2 is the temperature on the free surface, Q_2 is the corresponding calculated heat flux). The integral over all surfaces indicates that the thermal imbalance in the system is $(|Q_1 - Q_2|/Q_1) \times 100 = 1.07 \cdot 10^{-12}\%$, which indicates a high accuracy of the numerical calculation and a high quality of the generated computational grid.

Validation of 3-D modelling was controlled in two ways - by bringing together the heat balance and the water balance. For our case, checking the heat balance is a comparison of the values of heat flux through the heated and cold boundaries of the computational domain. At the heated boundary of the computational domain, the magnitude of the heat flux is set with a total power of 1290 W. Heat is removed through the inlet/outlet openings for the cooling water system going to the thermostat, as well as through radiation heat exchange from other surfaces (copper flanges, parts of CVD-diamond foil and the edges of the interlayer from liquid metal). The integral over all surfaces shows the magnitude of the thermal imbalance in the system; it does not exceed 0.000001%. The imbalance of mass water was carried out through control of the cooling water passing through the inlet and outlet openings. The mass imbalance was less than 0.049%.

3 Numerical modeling of thermal gravitational-capillary convection in FC-72

Fig. 2 shows the temperature isolines for a liquid with the Pr number=12.3 (Fluorinert Electronic Liquid FC-72). Due to the large value of $\Gamma = 100$, only a part of the region 16 mm $\leq x \leq$ 20 mm is shown in the figure. All regimes from $\Delta T = 0.1°$C to $\Delta T = 30°$C and higher are stationary. The Marangoni numbers characterizing thermocapillary convection significantly exceed the Grashof numbers responsible for thermogravitational convection. The liquid flow in a thin layer heated from below is characterized by small Grashof numbers. Thus, the flow has a pronounced thermo-

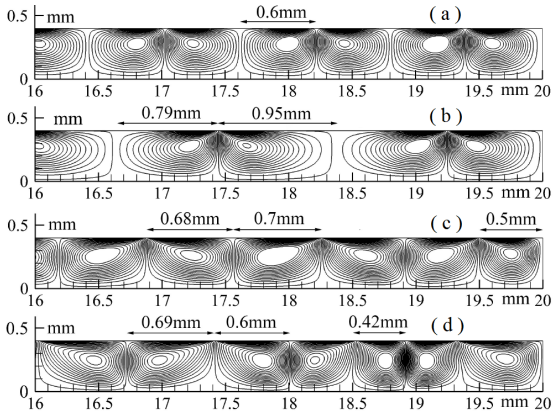

Figure 3: Fluorinert Electronic Liquid FC-72. $\Gamma = D/H = 100$. Isolines of the stream function of the plane $y = 0$. a) $\Delta T = 4°C$, Ra = 333, Ma = 7161; b) $\Delta T = 10°C$, Ra = 833, Ma = 17903; c) $\Delta T = 20°C$, Ra = 1667, Ma = 35806; d) $\Delta T = 30°C$, Ra = 2500, Ma = 53709.

capillary character: the ratio of the Ma/Gr numbers ≈ 264. When the temperature difference is $\Delta T \leq 3°C$, the temperature distributions in the liquid layer completely coincide with the heat conduction regime (Fig. 2a). Stable stratification by layer height is observed. Nusselt numbers, characterizing the relative contribution of convection and thermal conductivity to heat exchange, are of the order of 1.0. With an increase in temperature difference to $\Delta T = 3.1°C$ and higher, the temperature field undergoes significant changes (Fig. 2), convection already begins to contribute to heat exchange. The flow in a thin layer of Fluorinert Electronic Liquid FC-72 is laminar, stationary and axisymmetric.

Fig. 3 shows ordered Rayleigh-Benard convection cells in the form of ring shafts. At a temperature difference of $\Delta T = 4°C$, the cell sizes are almost the same and are about 0.6 mm (Fig. 3a). With an increase in the temperature difference, the size of the Rayleigh-Benard convection cells changes and becomes less uniform, the sizes are shown in Figs. 3b, 3c, 3d. Below we compare these sizes with the sizes of convection cells for water.

4 Numerical modeling of convection in water and comparison with FC-72

For water, the temperature difference between the heated bottom of the cylindrical layer and the free surface varied from 1°C to 20°C. If we set the temperature at the lower boundary to 85°C, this will be the temperature at which the researchers [17,19] studied the monolayer of levitating liquid microdroplets. First, the results are shown for a fixed height $H = 0.4$ mm and the ratio $\Gamma = D/H = 100$.

When the temperature difference is $\Delta T < 4.0°C$, the temperature distributions in the liquid layer completely coincide with the heat conduction mode (Figure 4a). For FC-72 liquid, this difference is $\Delta T < 3.1°C$ (Fig. 2). In these modes, stable stratification by layer height is observed. The Nusselt numbers, characterizing the

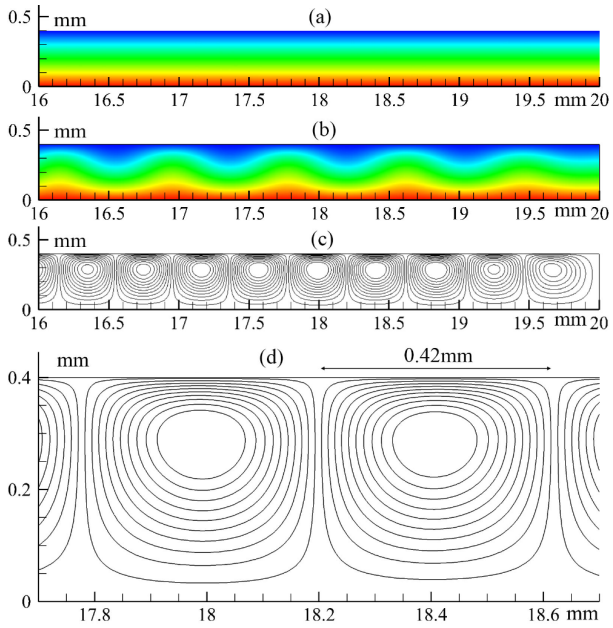

Figure 4: Water. $\Gamma = D/H = 100$. Stationary modes: a) Temperature isolines $T(x, z)$ in the section of the plane $y = 0$, $\Delta T = 3°C$, Ra = 10.0, Ma = 4077; b) Temperature isolines $T(x, z)$ in the section of the plane $y = 0$, $\Delta T = 4°C$, Ra = 28.2, Ma = 5396; c), d) isolines of the stream function in the section of the plane $y = 0$, $\Delta T = 4°C$, Ra = 28.2, Ma = 5396.

relative contribution of convection and heat conduction to heat transfer, are of the order of 1.0, which corresponds to the heat conduction mode. Convection is weakly expressed: the maximum flow velocity in the section $z = H/2$ is $5 \cdot 10^{-5}$ mm/s (for FC-72, the $\Delta T = 3.0°C$ mode, the maximum velocity amplitude was $1.5 \cdot 10^{-4}$ mm/s).

The Grashof number determines the intensity of thermogravitational convection. With a temperature difference of $\Delta T = 4$ and a layer height of $H = 0.4$ mm, the Grashof number will be $Gr = 13.1$. At the same time, the Marangoni number, which characterizes the contribution of thermocapillary convection to the flow structure, is several orders of magnitude greater than the Grashof number: Ma = 5390. Thus, in thin layers of liquid (water and FC-72) with a free surface, heated from below, convection has a pronounced thermocapillary character.

At the temperature difference $\Delta T = 4°C$ the temperature field undergoes significant changes (Figure 4b), convection already begins to contribute to heat exchange. The flow in a thin liquid layer is still laminar, stationary and axisymmetric. Rayleigh-Benard cells are clearly observed – ordered convective cells in the form of annular shafts, the cross-section of which is shown in Figure 4c. The cell size is about 0.42 mm (Fig. 4d). Compared to the mode with the temperature difference $\Delta T = 3°C$, the maximum velocity amplitude in the section $z = H/2$ has increased by almost 25,000 times and is already 1.09 mm/s (for FC-72, the $\Delta T = 3.1°C$ mode, the maximum velocity amplitude was 0.26 mm/s, which is more than 4 times lower than for water).

The flow regime with a temperature difference $\Delta T = 9.3°C$ (Gr = 28, Ma = 12066) for water is the last stationary and laminar regime. The convection intensity has

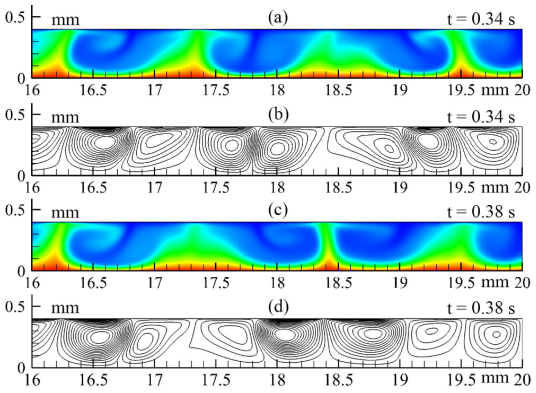

Figure 5: Water. Isotherms and isolines of the stream function in the section of the plane $y=0$, $\Gamma=D/H=100$. Non-stationary mode: $\Delta T=20°$C, Gr$=50.5$, Ma$=23970$: a), b) $t=0.3362$ s, c), d) $t=0.3762$ s.

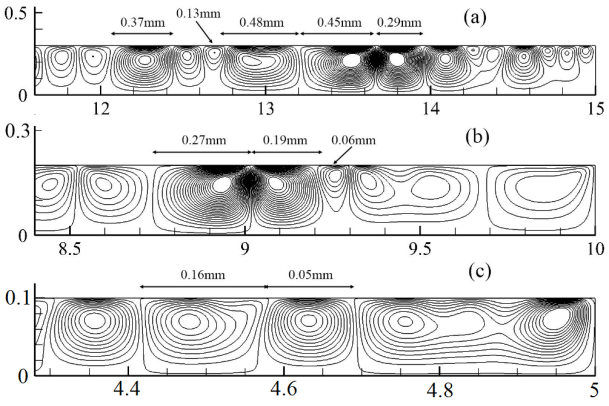

Figure 6: Water. Isolines of the stream function in the section of the plane $y=0$, $\Gamma=D/H=100$. Stationary modes. a) $\Delta T=3°$C, $H=0.3$ mm, $D=30$ mm, Gr$=4.2$, Ma$=3057$; b) $\Delta T=2°$C, $H=0.2$ mm, $D=20$ mm, Gr$=0.85$, Ma$=1369$; c) $\Delta T=1°$C, $H=0.1$ mm, $D=10$ mm, Gr$=0.05$, Ma$=345$.

increased significantly, the maximum velocity amplitude in the section $z = H/2$ is almost 10.5 mm/s. The shape of the isotherms changes significantly relative to the heat conduction regime due to thermocapillary flow, cold liquid is transferred from the surface to the lower part of the volume. Unlike water, for FC-72 liquid all regimes up to $\Delta T = 20°$C and higher are stationary.

With an increase in temperature difference by only 0.1°C, the flow loses stability. At $\Delta T = 9.4°$C (Gr $= 28.3$, Ma $= 12200$), the flow becomes unsteady. Ordered Rayleigh-Benard convection cells in the form of ring shafts begin to oscillate slightly in the radial direction. With an increase in temperature difference, at $\Delta T = 20°$C (Pr $= 2.39$, Gr $= 50.5$, Ma $= 23970$) (Fig. 5), the convection cells lose their uniform shape. Quite strong oscillations are observed here. The shape of the isotherms has changed even more compared to the heat conduction mode (Figs. 5a and 5c). At the same time, the flow of FC-72 liquid up to a temperature difference of ΔT$=30°$C and higher remains laminar and steady.

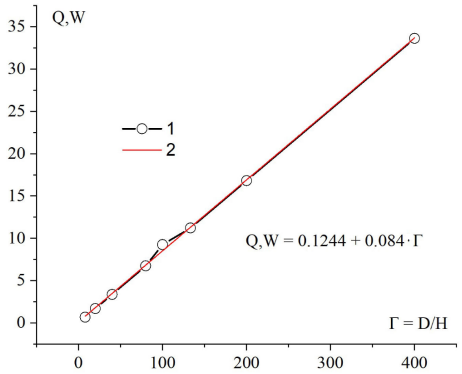

Figure 7: Water. 1 – Dependence of heat flux from the free surface on the height of the water layer; 2 – approximation by the function $y = a + xb$, $8 \leq \Gamma = D/H \leq 400$, $\Delta T = 4°C$, $D = 40$ mm.

The size of convective cells (water) varies from 0.48 mm to 0.69 mm, the cell sizes for FC-72 liquid change depending on the mode from 0.42 mm to almost 1 mm (Fig. 3). At large temperature differences, the thermocapillary flow transfers cold liquid from the surface almost to the very bottom. The integral heat transfer from the free surface of water in the $\Delta T = 20°C$ mode is almost 216 W. For FC-72 liquid, at a similar temperature difference, the integral heat transfer from the free surface is significantly less and is about 22 W. The value is calculated automatically in the Ansys Fluent software package.

Convection studies for water for a fixed value of $\Gamma = D/H = 100$ were also presented. The water layer diameter varied from 10 to 40 mm, and the water layer thickness, accordingly, varied from 0.1 to 0.4 mm. Fig. 6 shows the Rayleigh-Benard convection cells and their sizes. All modes were stationary. It is evident that with a decrease in the diameter of the thin water layer, the convection cells have different sizes and shapes, in contrast to the same annular shafts at $D = 40$ mm and $H = 0.4$ mm (Figs. 4, 5). At $D = 30$ mm, the size of the convection cells varied from 0.1 to 0.5 mm. With a decrease in the layer diameter to 10 mm, the convection cells become more uniform, decreasing in size (Fig. 6c).

With decreasing layer diameter, at a constant value of $\Gamma = D/H = 100$, the influence of the thermocapillary effect increases. At the same time, heat transfer from the free surface decreases. According to numerical calculations, with a layer diameter of $D = 40$ mm, the integral heat transfer was $Q = 8.4$ W, with a layer diameter of $D = 30$ mm - $Q = 4.7$ W, $D = 20$ mm - $Q = 2.1$ W, $D = 10$ mm - $Q = 0.5$ W. Heat transfer from the free surface is well approximated by a second-degree polynomial $Q = -0.0128 + 0.0016D + 0.005D^2$. The flow is entirely thermocapillary in nature, the contribution of buoyancy forces is insignificant, this is evident from the ratio of numbers Ma/Gr = 475. If we switch off thermocapillary convection by replacing the free surface with a rigid wall, then the water flow in the cylindrical cell will practically cease, and the isotherms will completely coincide with the thermal conductivity regime, as in Fig. 4a.

In the research the heat transfer patterns in extremely thin liquid layers were also studied. Fig. 7 shows the effect of the water layer height H on heat transfer, $8 \leq \Gamma =$

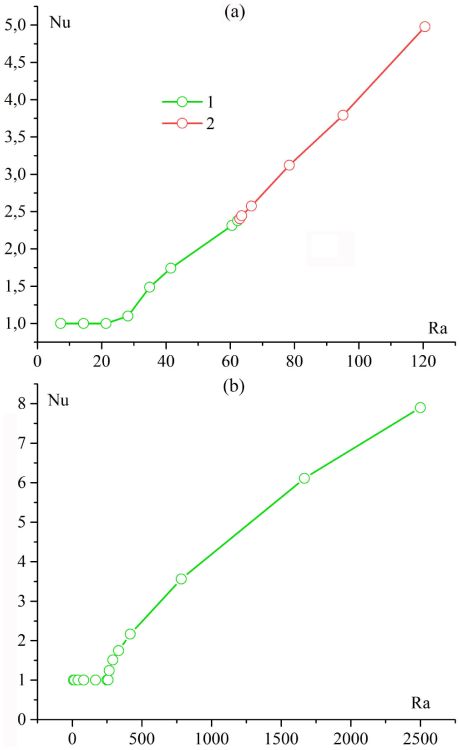

Figure 8: Dependence of integral heat transfer from the free surface on the Rayleigh number ($H = 0.4$ mm, $\Gamma = D/H = 100$). a) Water. 1 – stationary, laminar modes, 2 – non-stationary modes (in non-stationary modes Nu – time-averaged values); b) Fluorinert Electronic Liquid FC-72. Stationary, laminar modes.

$D/H \leq 400$. The temperature difference $\Delta T = 4°$C. The liquid layer height varied from 0.1 mm to 5 mm, the water layer diameter was fixed and was $D = 40$ mm. It is seen that heat transfer from the free surface increases almost linearly with increasing parameter $\Gamma = D/H$ and is well approximated by the function Q, $W = 0.1244+0.084\Gamma$. At the same time, with a decrease in the water layer height, the influence of the thermocapillary effect on the formation of the flow structure increases according to a cubic dependence. Thus, at a layer height $H = 5$ mm, the ratio Ma/Gr = 3, at a layer height $H = 1$ mm, the ratio Ma/Gr = 66, and at a layer height $H = 0.1$ mm ($\Gamma = D/H = 400$), the ratio Ma/Gr = 6420. Thus, as the layer height H decreases, at a fixed water layer diameter D, thermocapillary convection makes the main contribution to the formation of the flow structure and heat exchange.

Fig. 8 shows the dependences of the integral Nusselt number for water and FC-72 on the Rayleigh number. The Nusselt number characterizes the relative contribution of convection and thermal conductivity to heat exchange in the system. When the Nu number is close to 1.0, heat exchange occurs only due to the thermal conductivity of the liquid. With an increase in the temperature difference, the Nusselt number and the contribution of convection to heat exchange increase. In non-stationary modes for water, the Nusselt number is a time-averaged value. In numerical calculations in all modes, the imbalance of the heat flow through the heated and cold boundaries of the cylindrical region was less than 10-11. If we compare the relative contribution of

convection and thermal conductivity to heat exchange, i.e. Nusselt numbers for water and FC-72 liquid, it is clear that with the same Ra numbers, convection in FC-72 liquid makes a slightly more significant contribution to heat exchange (higher than the Nusselt number) compared to convection in water.

For FC-72 liquid, the dependence of the integral heat flow, measured in watts, from the free surface on the Rayleigh number is almost linear and is well approximated by the formula Q, $W = -1.666 - 0.00215\mathrm{Ra}$. The layer thickness H is 0.4 mm, $\Gamma = D/H = 100$.

4 Conclusion

Numerical study of thermal gravity-capillary convection in thin cylindrical layers of water and Fluorinert Electronic Liquid FC-72 with a height of 0.1 mm to 5 mm (aspect ratio $\Gamma = D/H$ up to 400), uniformly heated from below, is presented. These two liquids with significantly different thermophysical properties were chosen to better understand and generalize the regularities of convective flow and heat transfer in extremely thin layers. Differences in the sizes of convective cells for water and FC-72 are shown. It is shown that in both liquids the flow has a pronounced thermocapillary character. In a thin cylindrical layer of water $H = 0.4$ mm ($\Gamma = D/H = 100$) at temperature differences $\Delta T < 4$°C and in FC-72 liquid at temperature differences $\Delta T < 3.1$°C the temperature distributions in the thin layer coincide with the heat conduction regime. Compared with the temperature difference $\Delta T = 3$°C, at the temperature difference $\Delta T = 4$°C the maximum amplitude of the water flow velocity in the section $z = H/2$ increases by 24,000 times. For the regimes (water – $\Delta T = 4.0$°C, FC-72 – $\Delta T = 3.1$°C), when the temperature distribution in the layer of both liquids for the first time ceases to coincide with the heat conduction regime, the maximum velocity amplitude in water is more than 4 times higher than in FC-72. For water, the temperature difference ($\Delta T = 9.4$°C) was found when the flow becomes unsteady. It is shown that for a fixed diameter of the water layer, with a decrease in the height of the liquid layer, the influence of the thermocapillary effect increases in the form of a cubic dependence.

An analytical approximation of the dependence of the integral heat transfer from the free surface on the Rayleigh number for both liquids was presented. It was shown that, for the same Ra numbers, convection in the FC-72 liquid makes a slightly more significant contribution to heat transfer (higher than the Nusselt number) compared to convection in water. The diameter and height of the liquid layer, as well as the temperature differences, were chosen to be typical for experimental studies in which a monolayer of levitating microdroplets above the surface of a horizontal liquid layer was considered when heated by a localized heat source of different sizes [17,19]. In experimental studies of a monolayer of levitating water microdroplets, it was found that its dimensions can vary from 0.15 mm to 2.8 mm [17,41]. In this case, the number of microdroplets in clusters of the minimum size is 2-3 pieces. Numerical calculations show that the size of convective cells in a heated horizontal layer of water varies from 0.06 to 0.48 mm, i.e. it is quite comparable with the size of a monolayer of levitating microdroplets of water with a small number of them. Thus, the formation of convective cells

in a heated layer of liquid may well influence the monolayer of levitating microdroplets, i.e. determine its maximum size and the nature of its movement along the heated layer. Further research is needed to clarify all possible details of this effect.

In this research, the calculations concerned only convection in a very thin layer. Droplet formation and levitation are planned for future studies. In all theoretical and experimental works known to us on the study of a levitating array of droplets, the flow of evaporating liquid is considered uniform. The effect of non-uniformity of the vapor flow from the free surface of the liquid on the dynamics of a levitating droplet cluster has not yet been systematically studied. The study of the effect of non-uniformity of the vapor-gas flow on the dynamics of a levitating array of droplets is also beyond the scope of this research.

Acknowledgement

This work was supported by the Russian Science Foundation (Project No. 23-29-00919).

References

[1] Stone H., Stroock A., Ajdari A., *Engineering flows in small devices: Microfluidics Toward a Lab-on-a-Chip Annu*, Rev. Fluid Mech., 36 (2004), 381-411, DOI 10.1146/annurev.fluid.36.050802.122124.

[2] Bhardwaj R., Agrawal A., *Tailoring surface wettability to reduce chances of infection of COVID-19 by a respiratory droplet and to improve the effectiveness of personal protection equipment*, 32.8 (2020), 081702, DOI 10.1063/5.0020249.

[3] Mirskaya E., Agranovski I., *Generation of bacterial aerosols by interaction of microbial suspension with hot surfaces*, Journal of Aerosol Science 107 (2017), 1-8, DOI 10.1016/j.jaerosci.2017.02.001.

[4] Netz R., *Mechanisms of Airborne Infection via Evaporating and Sedimenting Droplets Produced by Speaking*, The Journal of Physical Chemistry B, 124.33 (2020), 7093-7101, DOI 10.1021/acs.jpcb.0c05229.

[5] Ajaev V., Kabov O., *Levitation and Self-Organization of Droplets*, Annual Review of Fluid Mechanics, 53 (2021), 203-225, DOI 10.1146/annurev-fluid-030620-094158.

[6] Schaefer V., *Observations of an early morning cup of coffee*, Am. Sci., 59.5 (1971), 534-535.

[7] Stefan, J., *Versuche uber die verdampfung. Sitzungsberichte der kaiserlichen Akademie der Wissenschaften in Wien II*, 65 (1873), 385-423.

[8] Fedorets A., *Droplet Cluster*, JETP Letters, 79. 8 (2004), 372-374, DOI 10.1134/1.1772434.

[9] Fedorets A., Marchuk I., Kabov O., *Role of Vapor Flow in the Mechanism of Levitation of a Droplet Cluster Dissipative Structure*, Technical Physics Letters, 37.2 (2011), 116-118, DOI 10.1134/S1063785011020064.

[10] Fedorets A., Marchuk I., Kabov O., *Coalescence of a droplet cluster suspended over a locally heated liquid layer*, Interfacial Phenomena and Heat Transfer, 1.1 (2013), 51-62, DOI 10.1615/InterfacPhenomHeatTransfer.2013007434.

[11] Fedorets A., Marchuk I., Kabov O., *On the role of capillary waves in the mechanism of coalescence of a droplet cluster*, JETP Letters, 99.5 (2014), 266-269, DOI 10.1134/S0021364014050087.

[12] Zaitsev D.V., Kirichenko D.P, Ajaev V.S., Kabov O.A., *Levitation and Self-Organization of Liquid Microdroplets over Dry Heated Substrates*, Physical Review Letters, 119.9 (2017), 094503, DOI 10.1103/PhysRevLett.119.094503.

[13] Zaitsev D.V., Kirichenko D.P., Kabov O.A., Ajaev V.S., *Levitation conditions for condensing droplets over heated liquid surfaces*, Soft Matter., 17 (2021), 4623-4631, DOI 10.1039/d0sm02185g.

[14] Davis J.E., Kabov O.A., Zaitsev D.V., Ajaev V.S., *Heat transfer, vapor diffusion and Stefan flow around levitating droplets near a heated liquid surface*, J. Fluid Mech., 964 (2023), A3, DOI 10.1017/jfm.2023.351.

[15] Lyulin Y.V., Spesivtsev S.E., Marchuk I.V., Kabov O.A., *Study of dynamics of thin liquid layer breakdown under conditions of spot heating and formation of a droplet cluster*, Thermophysics and Aeromechanics, 24.6 (2017), 949-952, DOI 10.1134/S0869864317060154.

[16] Shatekova A.I., *Condensation growth of microdroplets levitating over a heated liquid film*, Journal of Physics: Conference Series. 1677.1 (2020), DOI 10.1088/1742-6596/1677/1/012096.

[17] Zaitsev D.V., Kirichenko D.P., Shatekova, A.I., Ajaev, V.S., Kabov, O.A., *Experimental and theoretical studies of ordered arrays of microdroplets levitating over liquid and solid surfaces*, Interfacial Phenomena and Heat Transfer, 6.3 (2018), 219-230. DOI 10.1615/InterfacPhenomHeatTransfer.2019029816.

[18] Kabov O.A., Zaitsev D.V., Kirichenko D.P., Ajaev V.S., *Interaction of levitating microdroplets with moist air flow in the contact line region*, Nanoscale Microscale Thermophys. Eng., 21 (2017), 60-69, DOI 10.1080/15567265.2017.1279249.

[19] Shatekova A.I., Zaitsev D.V., Kabov O.A., *Evolution of a structured monolayer of levitating microdroplets over a heated horizontal liquid film*, IOP Publishing IOP Conf. Series: Journal of Physics: Conf. Series, 1105 (2018), 012138, DOI 10.1088/1742-6596/1105/1/012138.

[20] Gershuni G.Z., Zhukhovitsky E.M., *Convective stability of an incompressible fluid*, Moscow, Nauka, 1972. (in Russian)

[21] Berdnikov V.S., Vinokurov V.A., Vinokurov V.V., *Features of convective heat transfer in mixed convection regimes in the Czochralski method with different effects of buoyancy forces and thermocapillary effect*, Journal of Physics Conference Series, 1382.1 (2019), 012003, DOI 10.1088/1742-6596/1382/1/012003.

[22] Getling A.V., *Formation of spatial structures of Rayleigh-Benard convection*, Advances in Physics. Sci., 161.9 (1991), 1-80. (in Russian)

[23] Getling A.V., *Rayleigh-Benard convection*, Moscow, Structures and dynamics, Editorial URSS, 1999. (in Russian)

[24] Berdnikov V.S., Getting A.V., Markov V.A., *Wavenumber selection in Rayleigh-Benard convection: experimental evidence for the existence of an inherent*, Experimental heat transfer, 3.3 (1990), 269-288, DOI 10.1080/08916159008946390.

[25] Berdnikov V.S., Kirdyashkin A.G., *The structure of free convective flow in a horizontal layer of liquid under various boundary conditions, The structure of the near-wall boundary layer*, Collection of scientific works, Novosibirsk, Institute of Physics of the Siberian Branch of the USSR Academy of Sciences, 1978, 4-45. (in Russian)

[26] Berdnikov V.S., Grishkov V.A, Kovalevskii K.Yu., Markov V.A., *Thermal imaging studies of the laminar-turbulent transition in the Rayleigh-Benard convection*, Optoelectronics Instrumentation and Data Processing, 48.3 (2012), 111-120, DOI 10.3103/S8756699012030144,

[27] Bailon-Cuba J., Emran M.S., Schumacher J., *Aspect ratio dependence of heat transfer andlarge-scale flowin turbulent convection*, J. Fluid Mech, 655 (2010), 152-173, DOI 10.1017/S0022112010000820.

[28] Scheel J.D., Kim E., White K.R., *Thermal and viscous boundary layers in turbulent Rayleigh-Benard convection*, J. Fluid Mech, 711 (2012), 281-305, DOI https://doi.org/10.1017/jfm.2012.392.

[29] Schlichting H., Gersten K., *Boundary Layer Theory*, 8th edn. Springer, 2000.

[30] Vynnycky M., Masuda Y., *Rayleigh-Benard convection at high Rayleigh number and infinite Prandtl number: Asymptotics and numerics*, Physics of Fluids, 25.11 (2013), 113602, DOI: 10.1063/1.4829450.

[31] Sakievich P.J., Peet Y.T., Adrian R.J., *Large-scale thermal motions of turbulent Rayleigh-Benard convection in a wide aspect-ratio cylindrical domain*, Intern. J. Heat Fluid Flow, 61 (2016), 183-196, DOI:10.1016/j.ijheatfluidflow.2016.04.011.

[32] Sakievich P.J., Peet Y.T., Adrian R.J., *Temporal dynamics of large-scale structures for turbulent Rayleigh-Benard convection in a moderate aspect-ratio cylinder*, J. Fluid Mech, 901 (2020), A31, DOI https://doi.org/10.1017/jfm.2020.588.

[33] Pandey A., Scheel J.D., Schumacher J., *Turbulent superstructures in Rayleigh-Benard*, Nature Communications, 9.1 (2018), DOI 10.1038/s41467-018-04478-0.

[34] Richard J.A.M. Stevens, Blass A., Xiaojue Zhu, Verzicco R., *Detlef Lohse, Turbulent thermal superstructures in Rayleigh-Benard convection*, Phys. Rev. Fluids. 3 (2018), 041501, DOI 10.1103/PhysRevFluids.3.041501.

[35] Smirnov S.I., Smirnov E.M., *Direct numerical modeling of the turbulent Rayleigh-Benard convection in a slightly tilted cylindrical container*, Scientific and Technical Journal of St. Petersburg State Polytechnic University, Physical and mathematical sciences, 13.1 (2020), 14-25 DOI: 10.18721/JPM.13102.

[36] Roshan S., Ravy S., Mahendra K.V., *Large-eddy simulation of Rayleigh-Benard convection at extreme Rayleigh numbers*, Physics of Fluids, 34 (2022), 075133, DOI 10.48550/arXiv.2204.03697.

[37] Wen-Feng Z., Jun C., *Large-scale structures of turbulent Rayleigh-Benard convection in a slim-box*, Physics of Fluids, 33.6 (2021), 065103, DOI 10.1063/5.0048775.

[38] Xiaojue Z., Varghese M., Richard J.A.M. Stevens, Roberto V., and Detlef L., *Transition to the Ultimate Regime in Two-Dimensional Rayleigh-Benard Convection*, Phys. Rev. Lett., 120 (2018), 144502, DOI 10.1103/PhysRevLett.120.144502.

[39] Vinokurov V.A., Vinokurov V.V., Marchuk I.V., Kabov O.A., *Numerical study of Rayleigh-Benard convection in thin cylindrical liquid layers*, Interfacial Phenomena and Heat Transfer, 12.4 (2024), 1-16, DOI 10.1615/InterfacPhenomHeatTransfer.2024051995.

[40] Vargaftik N.B., *Handbook on the thermophysical properties of gases and liquids*, Moscow: Nauka, 1972. (In Russian)

[41] Shatekova A.I., Zaitsev D.V., *Interdroplet distance in a 2D ordered array of microdroplets levitating over a heated liquid layer*, AIP Conference Proceedings. 2212.1 (2020), 1-5, DOI:10.1063/5.0001071.

V.V. Vinokurov,
Kutateladze Institute of Thermophysics SB RAS,
Lavrentiev av. 1, 630090 Novosibirsk, Russia,
Email: jetset.vlad@gmail.com,

V.A. Vinokurov,
Kutateladze Institute of Thermophysics SB RAS,
Lavrentiev av. 1, 630090 Novosibirsk, Russia,
Email: vva.itp.nsc@mail.ru,

I.V. Marchuk,
Kutateladze Institute of Thermophysics SB RAS,
Lavrentiev av. 1, 630090 Novosibirsk, Russia,
Email:: igmarchuk@gmail.com,

O.A. Kabov,
Kutateladze Institute of Thermophysics SB RAS,
Lavrentiev av. 1, 630090 Novosibirsk, Russia,
Email: okabov@gmail.com.

Received 20.08.2024, Accepted 10.10.2024